Field observations of swash zone infragravity motions and beach cusp evolution

Yolanda Ciriano,[1] Giovanni Coco,[2] K. R. Bryan,[3] and Steve Elgar[4]

Received 14 May 2004; revised 3 November 2004; accepted 16 December 2004; published 22 February 2005.

[1] Fluid flows consistent with low-mode edge waves were evident in video observations of swash motions during a field experiment in which beach cusps developed on an initially smooth beach. As beach cusps grew, energy lying along low-mode dispersion curves increased. The most energetic edge-wave propagation direction changed from upcoast to downcoast as the orientation of the cusp horns rotated. These observations suggest a coupling between morphodynamics and hydrodynamics, and are evidence that beach cusp evolution might control low-mode edge wave dynamics.

Citation: Ciriano, Y., G. Coco, K. R. Bryan, and S. Elgar (2005), Field observations of swash zone infragravity motions and beach cusp evolution, *J. Geophys. Res.*, *110*, C02018, doi:10.1029/2004JC002485.

1. Introduction

[2] Infragravity waves with periods of 20–300 s influence hydrodynamics [*Guza and Thornton*, 1985; *Herbers et al.*, 1995] and sediment transport [*Beach and Sternberg*, 1991; *Russell*, 1993] in the surf and swash zones. Theoretical studies suggest infragravity waves that are refractively trapped close to the shoreline (edge waves) may generate surf [*Holman and Bowen*, 1982] and swash zone [*Guza and Inman*, 1975; *Guza and Bowen*, 1981] morphology. On a beach with uniform slope β, the edge wave dispersion relationship is [*Eckart*, 1951]

$$L_e = \frac{g}{2\pi} T_e^2 (2n+1) \tan\beta, \tag{1}$$

where L_e and T_e are the alongshore wavelength and period of the edge waves, g is gravity, and n is the mode number. Edge waves are forced by incident swell and sea (waves with periods from about 5 to 20 s), with subharmonics (twice the period of the incident waves) the most easily excited in laboratory conditions [*Guza and Davis*, 1974]. Subharmonic edge waves have been hypothesized to imprint their alongshore nodal structure on the beach morphology, with nodes (antinodes) corresponding to beach cusp horns (bays), resulting in a rhythmic shoreline pattern [*Guza and Inman*, 1975]. Despite the success of this theory to predict beach cusp spacing [*Coco et al.*, 1999], significant subharmonic energy has not been detected during beach cusp formation [*Holland and Holman*, 1996; *Masselink et al.*, 2004], and theory has shown that friction in a natural surf zone is likely to suppress the subharmonic response [*Guza and Bowen*, 1976]. In contrast, observations [*Coco et al.*, 2003] and numerical model results [*Reniers et al.*, 2004] are consistent with the formation of rhythmic features owing to self-organization mechanisms involving feedbacks between flow, sediment transport, and morphology [*Werner and Fink*, 1993]. However, pre-existing beach cusps potentially can affect swash hydrodynamics by directly forcing infragravity motions via triad interactions [*Bowen*, 1997], by detuning the edge wave dispersion relationship [*Guza and Bowen*, 1981], and by scattering edge wave energy into other modes [*Chen and Guza*, 1998, 1999].

[3] Edge waves are ubiquitous in the surf zone [*Huntley et al.*, 1981; *Oltman-Shay and Guza*, 1987; *Howd et al.*, 1992; *Bryan and Bowen*, 1998; *Özkan-Haller et al.*, 2001]. In contrast, field observations of infragravity motions in the swash zone [*Guza and Thornton*, 1982; *Holman and Sallenger*, 1985; *Holland et al.*, 1995; *Raubenheimer and Guza*, 1996; *Ruessink et al.*, 1998; *Holland and Holman*, 1999; *Raubenheimer*, 2002] have not been used to show how the edge wave dispersion relationship might be modified by the presence of swash morphology. Here the interactions between swash zone infragravity motions and evolving beach cusps are investigated with field observations [*Burnet*, 1998; *Coco et al.*, 2003, 2004] obtained, before, during, and after beach cusp formation.

2. Field Experiment

[4] The experiment was undertaken on an ocean beach at the U.S. Army Corps Field Research Facility (Duck, North Carolina) to study the development of beach cusps (Figure 1). Beach cusps were not present at the beginning of the experiment because a storm smoothed the beach. Swash fluid flow was measured by continuously recording 2-hour videotapes during daylight hours. Digitized (2 Hz) images

[1]Departament de Física Aplicada, Universitat Politècnica de Catalunya, Barcelona, Spain.
[2]National Institute of Water and Atmospheric Research, Hamilton, New Zealand.
[3]Coastal Marine Group, Department of Earth Sciences, University of Waikato, Hamilton, New Zealand.
[4]Woods Hole Oceanographic Institution, Woods Hole, Massachusetts, USA.

0148-0227/05/2004JC002485$09.00

Figure 1. Beach cusps and swash circulation at Duck, North Carolina (photo by Steve Elgar).

were analyzed to derive swash front elevation time series along cross-shore profiles spaced every 5 m alongshore [*Burnet*, 1998; *Coco et al.*, 2003]. Beach morphology was surveyed over a region encompassing the upper beach and the swash zone that included the area covered by beach cusps. Net changes between subsequent surveys usually occurred between the mean swash elevation and the mean swash elevation plus 2 standard deviations.

[5] During the experiment (Figure 2), an initially alongshore uniform beach developed 0.25-m-high cusps with 32-m alongshore spacing that evolved to cusps with 25 m spacing and 0.5 m height. Surveys and video observations (19 swash elevation time series) were collected along a 90-m stretch of coast.

[6] Two other experiments (already reported by *Burnet* [1998] and *Coco et al.* [2003, 2004]) in which pre-existing beach cusps were flattened by a bulldozer on a limited control section also were conducted. Beach cusps present at the edge of the control section were left undisturbed, and the extent to which they might have affected swash flow circulation patterns is unknown. Analysis of those experiments (not presented) is in agreement with the findings for a beach smoothed by a storm reported herein, although trends and patterns are not as evident because of the limited growth of beach cusps, a more limited data set due to less frequent correspondence of video coverage and beach surveys, the complicating presence of bidirectional incident waves (not observed during the experiment reported herein), and, possibly, the influence of the beach cusps at the sides of the domain, at least during the initial stages of beach cusp formation.

3. Methods

[7] Swash frequency spectra with resolution of 0.001 Hz were estimated by averaging spectra from detrended and windowed (Hanning, 50% overlap) 7000-s-long time series of swash elevation. Wave number–frequency spectra were estimated from time series observed at many alongshore locations using the iterative maximum likelihood estimator (IMLE) [*Pawka*, 1983] for frequencies f up to 0.200 Hz (frequency resolution of 0.001 Hz) and alongshore wave numbers k up to 0.05 m^{-1} (wave number resolution of 0.0006 m^{-1}). The wave number–frequency spectra were then divided into three regions: (1) an area dominated by energy related to wind, leaky (waves that are not refractively trapped close the shoreline, and propagate to deep water), and high-mode edge waves whose limit is defined by the leaky wave dispersion relationship [*Ursell*, 1952] plus a wave number offset (δ = 0.006 m^{-1}) to account for the width of energy peaks and the difficulty to distinguish, at the shoreline, between leaky waves and high-mode edge waves, (2) an area characterized by low-frequency motions (f < 0.025 Hz), and (3) an infragravity area where low-mode edge waves can exist (0.025 < f < 0.070 Hz) [*Holland and Holman*, 1999]. Within the region where edge waves have been observed in the past [*Huntley et al.*, 1981; *Oltman-Shay and Guza*, 1987; *Howd et al.*, 1992; *Bryan and Bowen*, 1998], lines of energy were observed in some of the spectra. A least squares technique (described in Appendix A) was used to determine the dimensionless slope of and relative amount of energy (γ) along these lines.

[8] Theoretical dispersion relationships were evaluated using a numerical model that accounts for topography and alongshore currents [*Falqués and Iranzo*, 1992; *Howd et*

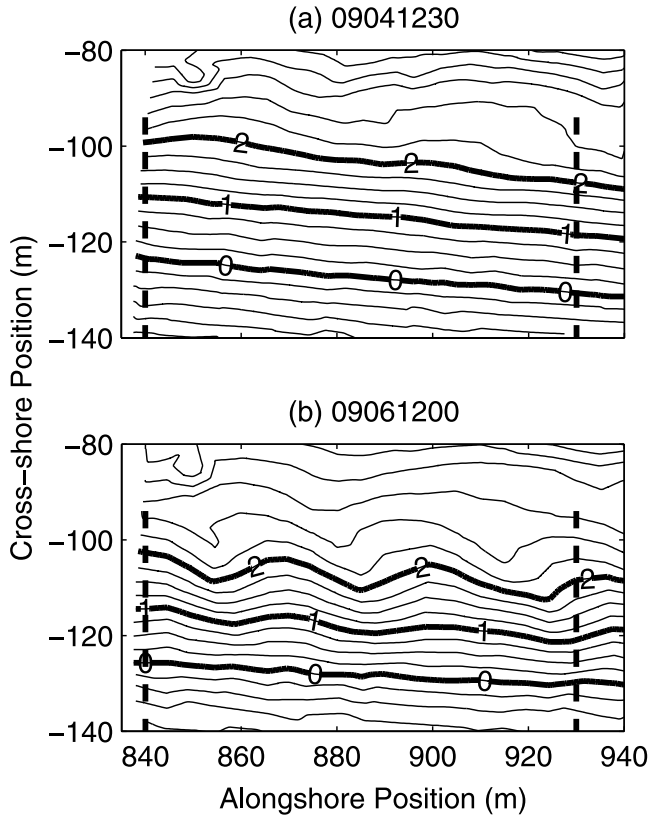

Figure 2. Contours of beach bathymetry (elevation relative to mean sea level) as a function of cross-shore and alongshore position. Seaward is toward more negative cross-shore positions. Dates are in the form"mmddhhhh" where mm is the month, dd is the day, and hhhh is the hour (local time) at the start of the survey. The section of beach covered by video observations is between the vertical dashed lines. Bold curves are 0-, 1-, and 2-m elevation contours.

al., 1992]. Large-scale bathymetry was estimated using a survey of the beach and surf zone obtained with an amphibious vehicle immediately after the experiment discussed here (the survey was performed on 7 September 1994). Observations from a cross-shore transect of current meters were used to estimate the alongshore current profile [*Feddersen et al.*, 1996]. The bathymetric survey (adjusted to account for the tidal level) and alongshore current measurements closest to the time the videotapes were recorded were used to estimate the theoretical edge wave dispersion relationships.

[9] Morphological parameters were evaluated only when the beginning of the video was within 3 hours of the survey. Beach cusp slope and orientation were measured inside an area defined by the mean swash elevation and the mean swash elevation plus 2 standard deviations. The location of horns (embayments) was determined by detecting maxima (minima) in the cross-shore position of a fixed elevation contour. This procedure was repeated at contours separated by 0.20 m to locate horns and embayments inside the area of interest. The slope of horns (embayments) was then estimated from a linear least squares fit to the elevation and cross-shore position of horns (embayments). The difference between the slope of beach cusp horns and bays, β_{BC}, was also calculated and considered as a measure of beach cusp size. Horn orientation θ was estimated as the difference between the overall beach orientation (given by the mean slope of a linear least squares fit to the cross-shore and alongshore position of surveyed points at a fixed elevation) and a linear least squares fit to the cross-shore and alongshore position of each horn location. An average horn orientation was assigned to each survey.

4. Observations

[10] Typical average swash elevation spectra obtained during the experiment are shown in Figure 3. The peak at the incident wind-wave frequency ($0.07 < f < 0.09$ Hz) can be detected for transects corresponding to either beach cusp horns or bays, but is more pronounced for time series collected in front of horns, similar to previous results [*Masselink et al.*, 1997]. Although the frequency of the swash flow is the same in horns and bays, a swash cycle in front of a steep beach cusp horn is stronger than in front of a bay where the up-rush is more likely to be attenuated by the interaction with the previous back-rush at a higher elevation [*Mase*, 1988]. At higher frequencies, energy decays with increasing frequency at a slower rate than previously observed [*Huntley et al.*, 1977; *Guza and Thornton*, 1982; *Mase*, 1988; *Ruessink et al.*, 1998].

[11] Wave number–frequency spectra (Figure 4) show that most of the energy is concentrated in the wind-wave frequency band. However, both leaky and nonleaky infragravity energy are present. The nonleaky infragravity contribution is somewhat consistent with the numerical prediction of a mode-zero edge wave dispersion relationship (Figure 4), although the degree of consistency varied during the experiment.

[12] During the experiment, incident wave ($0.05 < f < 0.25$ Hz) significant height decreased from about 2 to 1 m, mean alongshore currents in 4-m water depth ranged from 0.05 to 0.35 m/s, and total swash energy was tidally

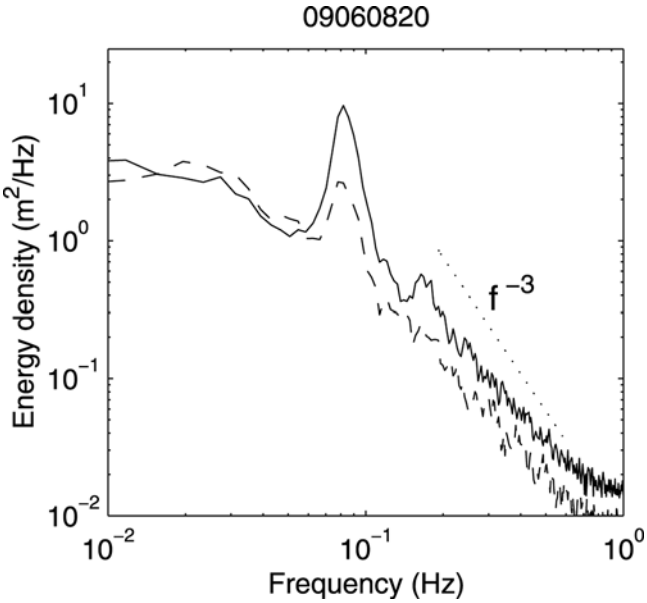

Figure 3. Energy density versus frequency from swash elevation time series in horns (solid curve) and bays (dashed curve). Spectra corresponding to three horn and two bay time series have been averaged. The dotted line is high-frequency saturation decay f^{-3}. There are approximately 108 degrees of freedom in the spectral estimates.

modulated (Figures 5a, 5b, and 5c). Relative energy in the wind-wave (infragravity) region decreased (increased) on falling tide and vice versa on rising tide (Figures 5d and 5e), similar to previous results [*Wu et al.*, 1985]. Similar to the wind-wave relative energy, beach cusp slope (and thus, beach cusp height) (Figure 5f) increased (decreased) during falling (rising) tide [see also *Coco et al.*, 2004]. Assuming the lines of energy in wave number–frequency spectra (Figure 4) are edge waves, dispersion relationships determined by regression lines with slope β_{rl} (Figure 5h) were identified in each of the nine videotapes analyzed during the experiment. (There was no significant evidence of northward propagating edge waves at 1800 hours on 6 September) The slope of edge wave dispersion lines varied with the tide (Figure 5h), although not as predicted by the numerical simulations (Figure 5i). Furthermore, concomitant with the rotation of horn orientations (Figures 5g and 6), more energy was associated with the positive wave number mode (northward propagation) during the first tide (positive beach cusp horn orientation) and with the negative wave number mode (southward propagation) during the second (negative beach cusp horn orientation).

5. Discussion

[13] Wave number–frequency spectra of swash elevation time series observed during beach cusp formation indicate the presence of fluid motions characterized by a dispersion relationship indicative of low-mode edge waves. Differences between the energy-weighted, zero-forced, regression lines in the wave number–frequency domain and numerical predictions using a model that accounts for the effects of cross-shore variations to alongshore currents and bathyme-

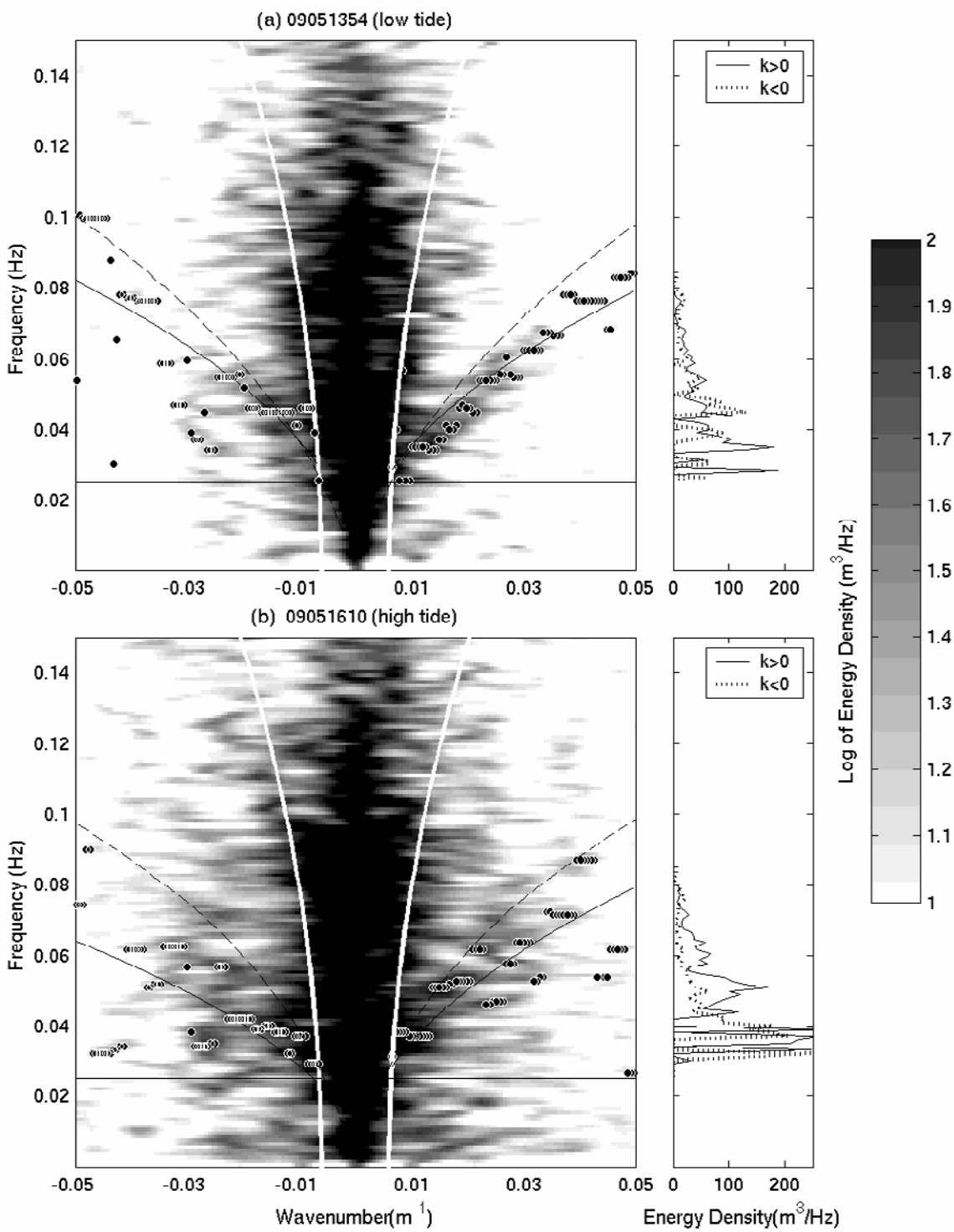

Figure 4. Wave number-frequency spectra of swash elevation time series evaluated at (a) low (09051354) and (b) high (09051610) tide. Grayscale represents energy density levels on a log scale (shown on the right side). Leaky and high-mode edge waves fall between the white curves, and low-mode edge waves fall between the white curves and the horizontal solid lines. Dashed black curves indicate numerical model predictions of mode-zero edge waves. Circles show the energy maximum at each wave number within the edge wave area. Solid curves show the energy-weighted, zero-forced regressions. The panels on the right side indicate the maximum energy density along these regression curves (see Appendix A) for positive (solid curves) and negative (dashed curves) wave numbers. Energy contributions leaking from the gravity band have not been included (see Appendix A). There are approximately 14 degrees of freedom in the spectral estimates. Beach cusp slope (β_{BC}) is equal to 0.20 at low tide and equal to 0.08 at high tide.

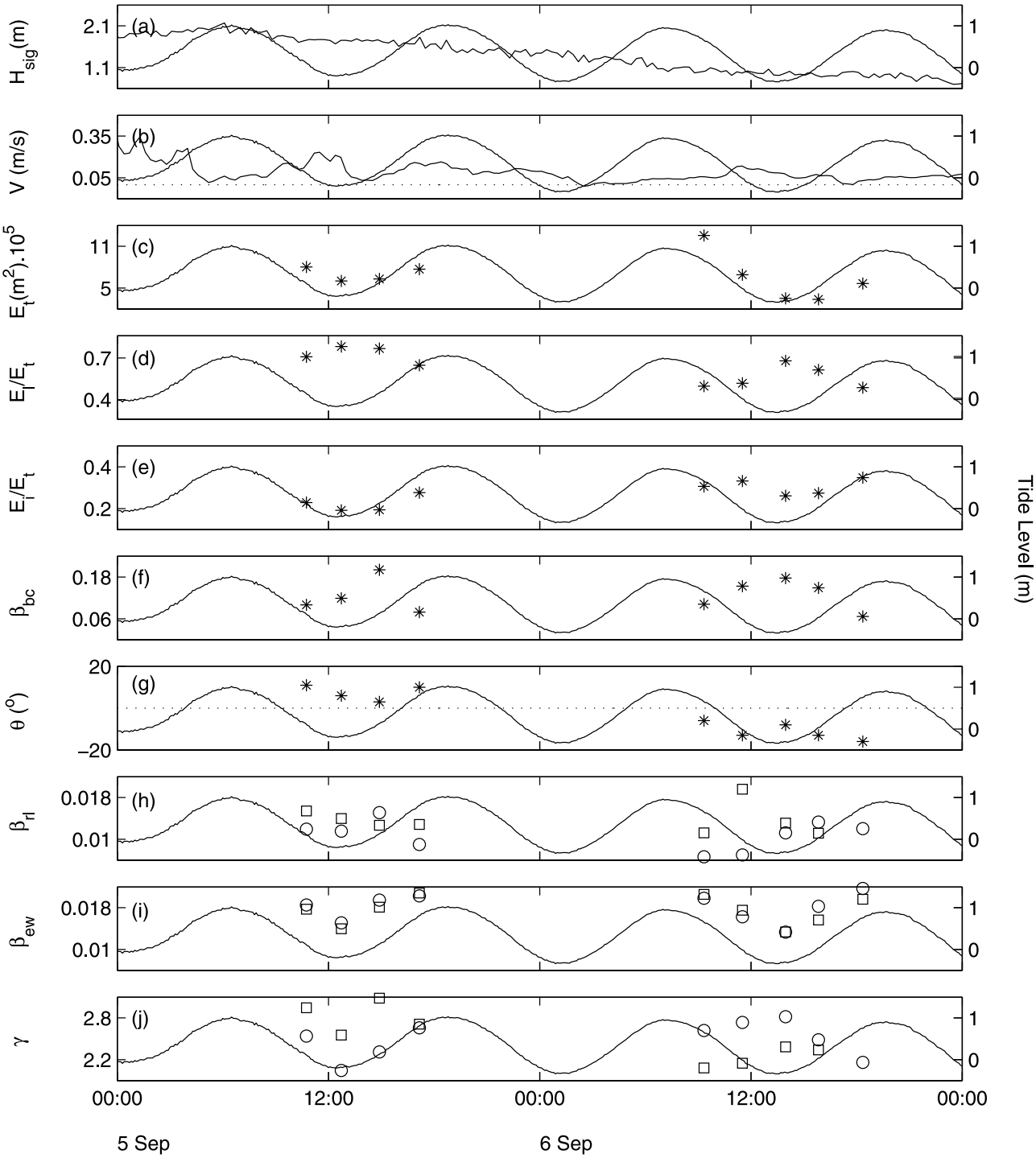

Figure 5. Hydrodynamic and morphological parameters versus time. The solid curve in each panel is tide level. (a) Significant wave height and (b) alongshore current velocity. Values are averages over 1024 s from a colocated pressure gauge and current meter in approximately 4-m water depth. (c) Total energy (integrated for wave numbers between -0.05 and 0.05 m^{-1}, and for frequencies between 0 and 0.07 Hz). Relative energy for the (d) leaky wave and (e) infragravity (up to 0.07 Hz frequencies) regions (note different scales). (f) Beach cusp slope (a surrogate for beach cusp height) and (g) beach cusp orientation (zero corresponds to beach normal and positive angles correspond to southerly beach cusp horn orientation). (h) Slope of energy-weighted, zero-forced, regression line. (i) Slope of mode zero edge wave dispersion relationship predicted by numerical model. Squares (circles) are positive (negative) wave numbers. (j) Relative energy corresponding to regression curve (see equation 2).

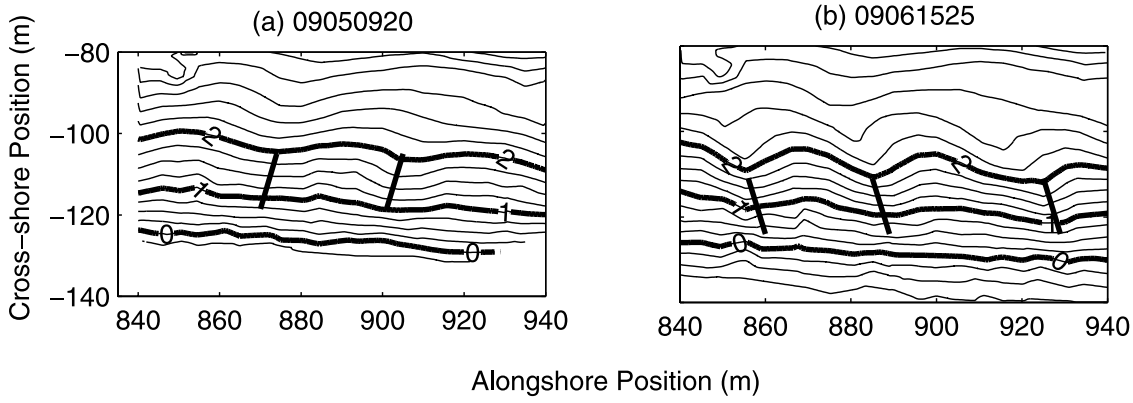

Figure 6. Contours of beach bathymetry as a function of cross-shore and alongshore position showing (solid lines) the average orientation of beach cusp horns of 11° ((a) 09050920) and, at the following tide, the average orientation of −13° ((b) 09061525). Positive (negative) angles correspond to southerly (northerly) beach cusp horn orientation. Bold curves are 0-, 1-, and 2-m elevation contours.

try [*Falqués and Iranzo*, 1992; *Howd et al.*, 1992] can be well above 50% (Figure 4). Such differences could not be related to the height or slope of the cusps, nor to tidal levels, but potentially could originate from approximations in the edge wave model, which is linear, does not account for swash zone morphology and circulation patterns, uses the average alongshore beach profile, does not consider alongshore current nonuniformity, and is sensitive to changes in the beach profile [*Bryan and Bowen*, 1998]. In addition, only one profile extending across the surf zone was available during the experiment, possibly resulting in errors in predictions of high-mode edge waves, which are sensitive to the location of a surf zone sandbar. Previous surf zone studies [*Huntley et al.*, 1981; *Oltman-Shay and Guza*, 1987, 1993; *Bryan and Bowen*, 1998] have shown favorable agreement of current meter data with numerical predictions of edge waves. Recent numerical modeling [*Reniers et al.*, 2004] suggests that the interaction between rhythmic surf zone morphology and incident waves forces the development of edge waves. Differences between observations and numerical predictions also could originate from the use of the IMLE technique with run-up observations. The IMLE might be affected by the presence of rhythmic cuspate features causing time lags between swash motions in cusp horns and bays [*Coco et al.*, 2003] that could increase concentration of energy at wave numbers related to the beach cusp spacing.

[14] An alternative explanation for the observed patterns in the infragravity wave number–frequency spectra is that swash run-up and run-down interact, generating energy at subharmonic frequencies [*Mase*, 1988]. The difference in beach slope between regularly spaced cusp horns and bays might cause energy to spread over a broad range of frequencies and wave numbers. Simulations using a ballistic model do not show energy in the wave number–frequency spectrum indicative of low-mode edge waves. Although the model makes many simplifying assumptions and the model results are preliminary, at this stage they are consistent with the conclusion that the dispersion lines might be low-mode edge waves, and not an artifact of obliquely incident waves propagating across a cuspate morphology. Further numerical modeling of flow over beach cusps and interactions between subsequent bores is needed to address this possibility.

[15] The observations suggest that the dispersion relationships estimated from wave number–frequency spectra are related to beach cusp evolution. A strong correlation between the orientation of beach cusps and the direction of propagation of the most energetic mode consistently was observed in the wave number–frequency spectra (Figure 7). For example, when beach cusps were oriented to the south (positive values of θ), wave modes were more likely to propagate to the south (positive wave numbers). The direc-

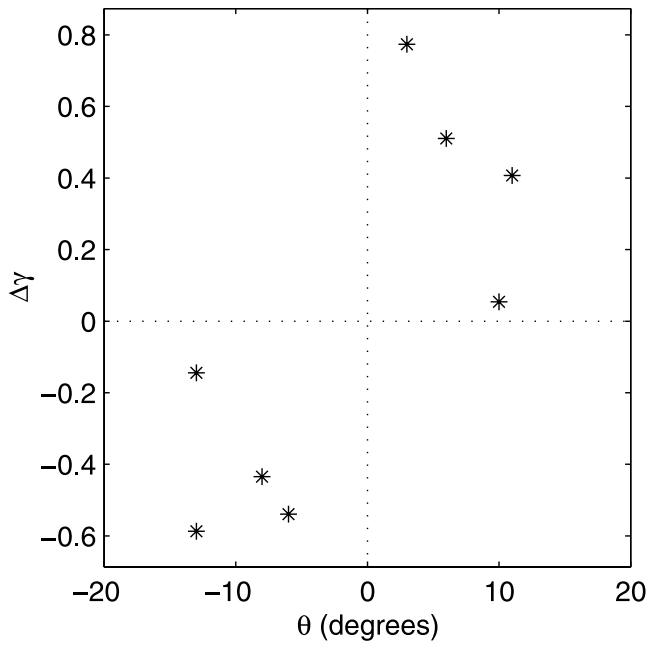

Figure 7. Difference in energy concentration Δγ between dominant modes in the positive and negative wave number domains (positive Δγ indicates that more energy can be associated with the positive, southward propagating, dominant mode) versus average beach cusp horn orientation θ (positive values of θ indicate a southward horn orientation).

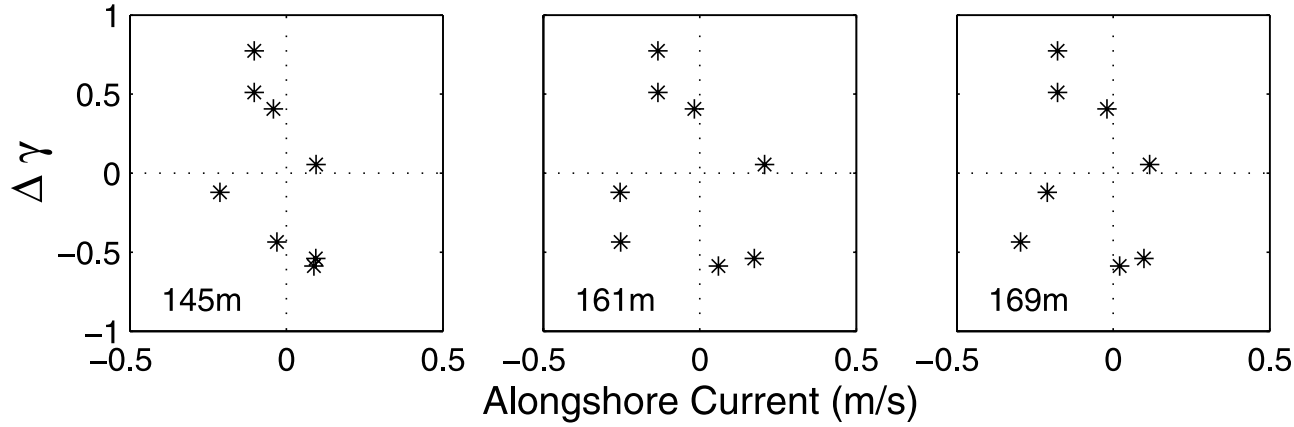

Figure 8. Difference in swash energy concentration $\Delta\gamma$ versus mean alongshore current for dominant modes in the positive and negative wave number domain. Alongshore current values are averages over 1024 s from a cross-shore transect of current meters (cross-shore position of each current meter is indicated in the lower left corner).

tion of propagation of the most energetic mode was not related to the observed alongshore currents (Figure 8). The change in orientation of beach cusp horns appears to be related to the tidally modulated reversal of the alongshore current already observed at Duck [*Wu et al.*, 1985], even though beach cusps are not observed to change their orientation every time the alongshore current reverses. Morphological changes occur more slowly than hydrodynamic changes, and thus the reversed alongshore current needs to be maintained long enough for beach cusps to change their orientation. In contrast, edge waves should readjust instantaneously to a reversal of the alongshore current. Observations from the most shallow water current meter (Figure 9) show an initially (09050600) strong (0.45 m/s) positive alongshore current that may be associated with the positive orientation of beach cusp horns. (Dates such as 09050600 are in the form"mmddhhhh" where mm is the month, dd is the day, and hhhh is the hour (local time) at the start of the survey.) The two subsequent periods of negative and positive alongshore current are of limited duration (09051200) or intensity (09051800), causing a limited effect on beach cusp horn orientation (Figure 5g) and on the direction of propagation of the most energetic mode. On the following high tide (09060300), there is a negative alongshore current of longer duration and intensity (−0.4 m/s) that could be responsible for the new orientation of beach cusp horns. The following positive alongshore current (09061200) is weak (<0.2 m/s), causing no change on the horn orientation. In this case, no changes in the direction of propagation of the most energetic mode were observed, in contrast to the hypothesis that the observed edge waves passively and instantaneously readjust to the alongshore current (which is the reason for the lack of a relationship in Figure 8 for the most shallow water current meter). Observations in deeper water (Figure 5b) do not show any change in the alongshore current direction.

[16] During the experiment, the relative amount of edge-wave energy increased 50% as the beach cusp size increased by a factor of 3 (Figure 10), energy associated with mode-zero edge waves was broad banded and tidally modulated and varied with changes in beach cusp size (Figure 5f), and the ratio of the most energetic mode-zero wave number to the beach cusp wave number tended to 0.5 for increasing beach cusp size (Figure 11).

[17] It has been hypothesized that even limited standing edge wave activity can lead to the appearance of beach cusps [*Inman and Guza*, 1982; *Coco et al.*, 2001]. At the beginning of the experiment, soon after the storm had smoothed a pre-existing cuspate morphology, a survey was conducted (starting on 09041230, Figure 2) and a videotape recorded (starting on 09041316). Analysis conducted of the first hour of video measurements (to minimize

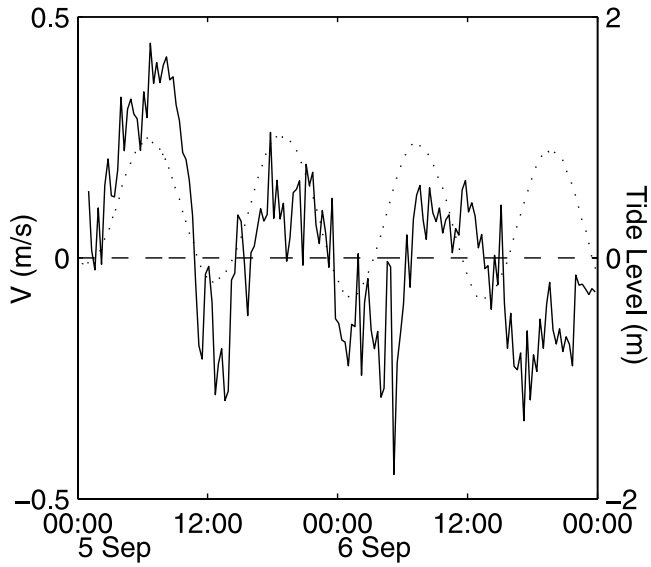

Figure 9. Tidal modulation of alongshore current velocity. Solid curve is the 1024-s average alongshore velocity observed in approximately 2-m water depth (cross-shore position is 145 m). The dotted curve is tide level at the same location as the velocity time series.

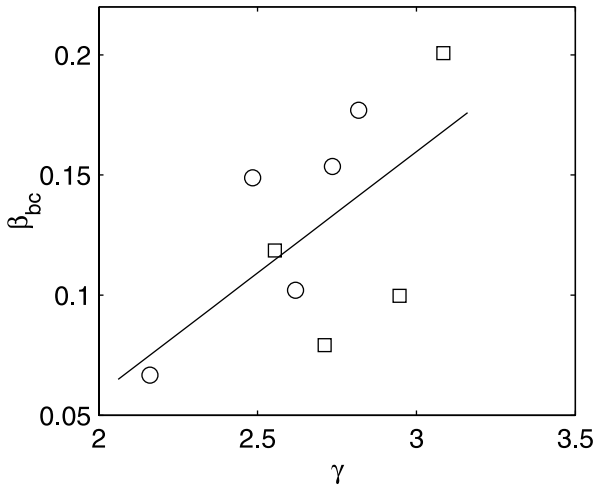

Figure 10. Beach cusp slope versus relative energy concentrated along the energy-weighted, zero-forced regression lines. The solid line is a linear least square regression (r = 0.60, significant at 95% level).

the effect of developing beach cusps) shows (Figure 12) a limited amount of relative energy in the infragravity region (below values observed in the remaining of the experiment) and no detectable edge wave signal at frequencies and wave numbers that could induce the beach cusp geometry later observed. Although this result does not provide conclusive evidence (no more surveys were performed that day, and as a consequence, no beach cusp growth rate could be inferred), edge wave energy was not observed during the initial stages of beach cusp formation.

[18] The mechanisms driving the observed fluid motions cannot be established unequivocally by these data. It is possible that bore interactions [*Mase*, 1988] or the presence of topographical perturbations caused low-frequency motions or even edge waves to occur, as observed in laboratory experiments [*Buchan and Pritchard*, 1995]. Another possible mechanism is backscattering of edge waves by rhythmic topography [*Chen and Guza*, 1998, 1999], although this theoretical approach does not account for beach cusp orientation. Moreover, the requirement of an incoming edge wave cannot be tested with the present data (an alongshore array of current meters would be required). The hypothesis [*Bowen*, 1997] that the relative proportion of edge wave energy increases with cusp size owing to nonlinear interactions between beach cusps and edge waves cannot be tested with these data owing to the lack of surf zone observations. Notwithstanding which mechanism is responsible, these observations indicate the presence of shoreline fluid motions characterized by a dispersion relationship indicative of low-mode edge waves, and that slowly evolving beach cusps and swash zone hydrodynamics at infragravity frequencies are coupled.

6. Conclusions

[19] (1) Wave number–frequency spectra of swash zone elevation time series indicate the presence of low-mode edge waves during a field experiment in which beach cusps developed from an initially smooth beach. (2) Predictions using a numerical model that accounts for the effects of alongshore currents and bathymetry generally do not reproduce the observed temporal changes in the edge wave dispersion relationships. (3) As beach cusps grew, edge wave energy increased, and the observations suggest that the most energetic mode of edge wave propagation was related to the orientation of beach cusp horns rather than to the alongshore current.

Appendix A: Detection of Edge Wave Dispersion Curves

[20] A procedure is outlined here to search wave number–frequency space for the maximum energy peaks in the region that might contain low-mode edge waves. This was designed to detect edge wave dispersion relationship without making any a priori assumption on the presence or modes of edge waves. The maximum energy was detected while holding the wave number k constant. Maxima related to energy peaks that lie inside the leaky wave region or on the separation between the leaky wave and infragravity regions were omitted. To separate energy peaks that might belong to different modes, clusters of energy peaks were isolated by plotting the ratio $f^2/(gk)$ against k for each peak, and separating those clusters characterized by a minimum distance $\delta(f^2/(gk))$ larger than 0.01. Clusters containing less than 5% of the total number of points were eliminated, and a new energy peak was detected from that wave number band in the original spectrum.

[21] An energy-weighted, linear regression of the energy peaks belonging to each cluster was used to identify a potential edge wave dispersion relationship. The regression was forced to go through the origin. The coefficient of determination for such regressions was evaluated according to *Gordon* [1981]. Regressions resulting in negative values indicate lack of significance and were discarded from subsequent analysis. Sometimes ridges of energy in the

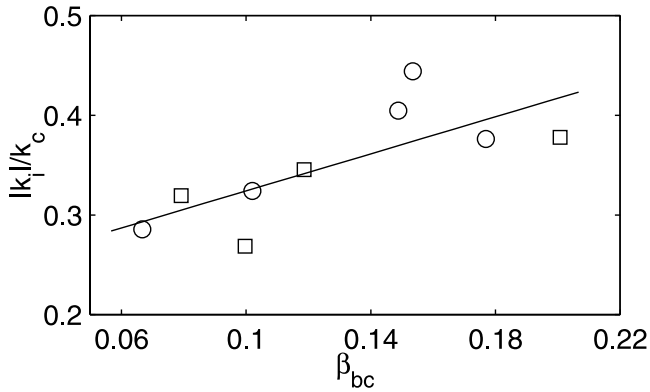

Figure 11. Ratio of the absolute value of the most energetic mode-zero wave number k_i to the beach cusp wave number k_c versus beach cusp slope (a surrogate of beach cusp height). Squares (circles) refer to positive (negative) wave numbers. The solid line is a linear least square regression (r = 0.74, significant at 95% level).

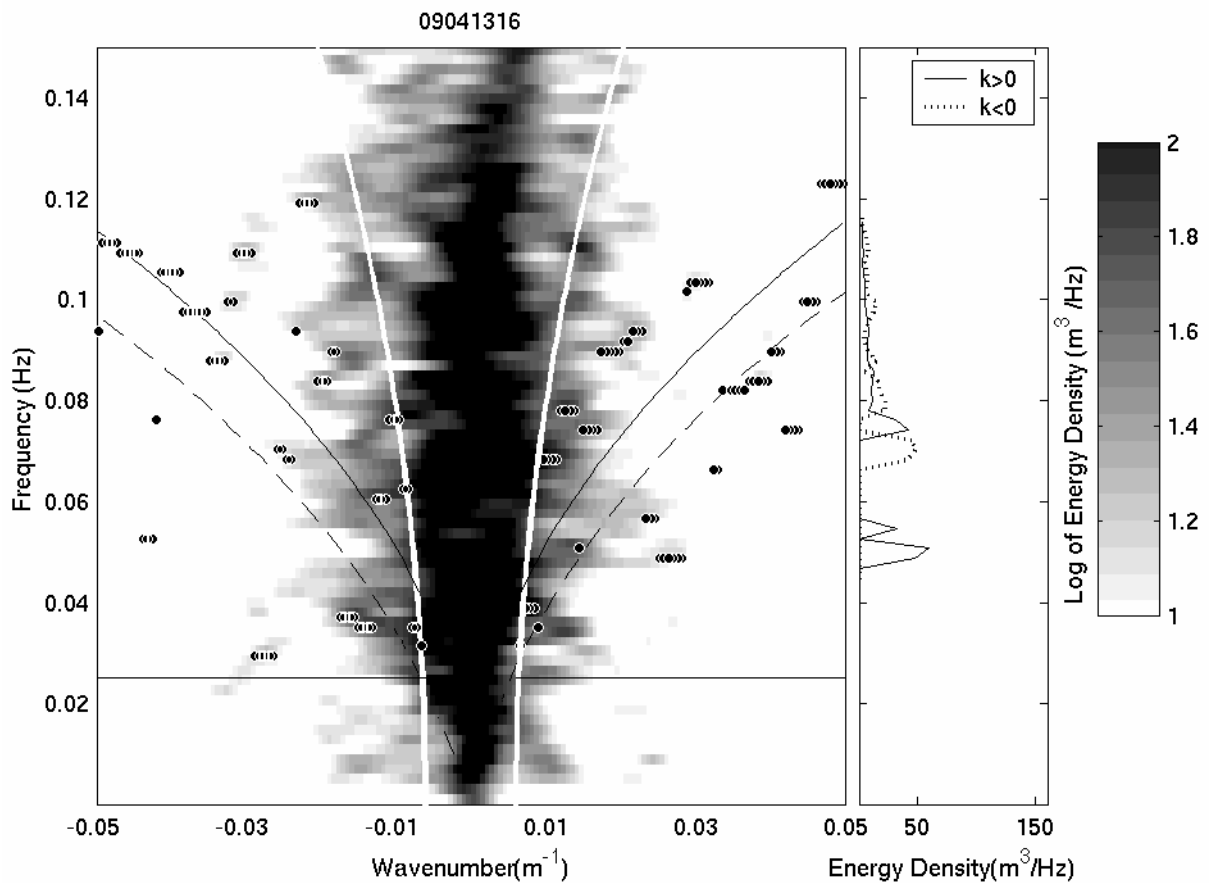

Figure 12. Wave number-frequency spectra of swash elevation time series evaluated at the beginning of the experiment (09041316). Grayscale represents energy density levels on a log scale (shown on the right). Leaky and high-mode edge waves fall between the white curves, and low-mode edge waves fall between the white curves and the horizontal solid lines. Dashed black curves indicate numerical model predictions of mode-zero edge waves. Circles show the energy maximum at each wave number within the edge wave area. Solid curves show the energy-weighted, zero-forced regressions. The panels on the right indicate the maximum energy density along these regression curves (see Appendix A) for positive (solid curves) and negative (dashed curves) wave numbers. Energy contributions leaking from the gravity band have not been included (see Appendix A). There are approximately 14 degrees of freedom in the spectral estimates.

spectrum appeared to extend to frequencies higher than 0.07 Hz, in which case the limit of the maximum frequency analyzed was extended upward. Energy density associated with each line (E_{rl}) was evaluated by summing energy levels within an area defined by the regression line, plus and minus 10 neighboring wave numbers (equaling the offset δ) and dividing by the number of points (n_{rl}). Energy density associated with regression lines obtained from different wave number–frequency spectra were compared using the parameter

$$\gamma = \frac{E_{rl}/n_{rl}}{E_i^*/n_i^*}, \tag{A1}$$

where E_i^* indicates the total energy present in a region bounded by the leaky wave dispersion relationship and $0.025 < f < 0.200$ Hz (this region accounts for edge wave dispersion relationships extending to frequencies higher than those of infragravity waves) and n_i^* indicates the number of points in the region. Physically, γ is a measure of how much energy lies on the regression line relative to the average energy present in the region of the wave number–frequency spectrum considered. This parameter, in comparison with others that relate the energy along the edge wave dispersion line with the total infragravity energy, has the advantage of not being sensitive to the observed tidal modulation in infragravity energy and so allows for comparisons between observations collected at any tidal stage.

[22] **Acknowledgments.** Planning and execution of the DozerDuck field experiment was led by B. T. Werner supported by an Office of Naval Research (ONR) Young Investigator Award (N00014-92-J-1446) and ONR, Coastal Dynamics. Field assistance from E. Gallagher, R. T. Guza, B. Raubenheimer, B. Scarborough, R. Whitsel, B. Woodward, J. Dean, M. Okihiro, S. Conant, W. Boyd, M. Clifton, and the staff of the U.S. Army Corps of Engineers Field Research Facility and data from the Duck94 Guza-Elgar-Herbers transect are gratefully acknowledged. Discussions with D. A. Huntley, R. T. Guza, A. Sheremet, B. Raubenheimer, A. Falqués, and two anonymous reviewers are gratefully acknowledged. This work was

performed while Y. C. was a visiting scientist at NIWA funded by UPC. Y. C. thanks NIWA for its kind hospitality. G. C. is supported by the (New Zealand) Foundation for Research, Science and Technology (contract C01X0401). S. E. was supported by ONR, NSF, and ARO.

References

Beach, R. A., and R. W. Sternberg (1991), *A note on modeling of turbulence in the surf zone, in Coastal Sediments '91: Proceedings*, edited by N. C. Kraus, K. J. Gingerich, and D. L. Kriebel, pp. 114–128, Am. Soc. of Civ. Eng., Reston, Va.

Bowen, A. J. (1997), Patterns in the water: Patterns in the sand?, in *Coastal Dynamics '97*, edited by E. B. Thornton, pp. 1–10, Am. Soc. of Civ. Eng., Reston, Va.

Bryan, K. R., and A. J. Bowen (1998), Bar-trapped edge waves and longshore currents, *J. Geophys. Res.*, *103*, 27,867–27,884.

Buchan, S. J., and W. G. Pritchard (1995), Experimental observations of edge waves, *J. Fluid Mech.*, *288*, 1–35.

Burnet, T. K. (1998), Field testing two beach cusp formation models, Ph.D. thesis, Duke Univ., N. C.

Chen, Y., and R. T. Guza (1998), Resonant scattering of edge waves by longshore periodic topography, *J. Fluid Mech.*, *369*, 91–123.

Chen, Y., and R. T. Guza (1999), Resonant scattering of edge waves by longshore periodic topography: Finite beach slope, *J. Fluid Mech.*, *387*, 255–269.

Coco, G., T. J. O'Hare, and D. A. Huntley (1999), Beach cusps: A comparison of data and theories for their formation, *J. Coastal Res.*, *15*(3), 741–749.

Coco, G., D. A. Huntley, and T. J. O'Hare (2001), Regularity and randomness in the formation of beach cusps, *Mar. Geol.*, *178*, 1–9.

Coco, G., T. K. Burnet, B. T. Werner, and S. Elgar (2003), Test of self-organization in beach cusp formation, *J. Geophys. Res.*, *108*(C3), 3101, doi:10.1029/2002JC001496.

Coco, G., T. K. Burnet, B. T. Werner, and S. Elgar (2004), The role of tides in beach cusp development, *J. Geophys. Res.*, *109*, C04011, doi:10.1029/2003JC002154.

Eckart, C. (1951), Surface waves on water of variable depth, *Wave Rep. 100*, pp. 51–12, Scripps Inst. of Oceanogr., La Jolla, Calif.

Falqués, A., and V. Iranzo (1992), Edge waves on a longshore shear flow, *Phys. Fluids A*, *4*(10), 2169–2190.

Feddersen, F., R. T. Guza, S. Elgar, and T. H. C. Herbers (1996), Cross-shore structure of longshore currents during Duck94, paper presented at 25th International Conference of Coastal Engineering, Am. Soc. of Civ. Eng., Sydney.

Gordon, H. A. (1981), Errors in computer packages: Least squares regression through the origin, *Statistician*, *30*(1), 23–29.

Guza, R. T., and A. J. Bowen (1976), Resonant interactions for waves breaking on a beach, paper presented at 15th International Conference of Coastal Engineering, Am. Soc. of Civ. Eng., Honolulu, Hawaii.

Guza, R. T., and A. J. Bowen (1981), On the amplitude of beach cusps, *J. Geophys. Res.*, *86*(C5), 4125–4132.

Guza, R. T., and R. E. Davis (1974), Excitation of edge waves by waves incident on a beach, *J. Geophys. Res.*, *79*(9), 1285–1291.

Guza, R. T., and D. Inman (1975), Edge waves and beach cusps, *J. Geophys. Res.*, *80*(21), 2997–3012.

Guza, R. T., and E. B. Thornton (1982), Swash oscillations on a natural beach, *J. Geophys. Res.*, *87*(C1), 483–491.

Guza, R. T., and E. B. Thornton (1985), Observations of surf beat, *J. Geophys. Res.*, *90*(C2), 3161–3172.

Herbers, T. H. C., S. Elgar, and R. T. Guza (1995), Generation and propagation of infragravity waves, *J. Geophys. Res.*, *100*(C12), 24,863–24,872.

Holland, K. T., and R. A. Holman (1996), Field observations of beach cusps and swash motions, *Mar. Geol.*, *134*, 77–93.

Holland, K. T., and R. A. Holman (1999), Wavenumber-frequency structure of infragravity swash motions, *J. Geophys. Res.*, *104*(C6), 13,479–13,488.

Holland, K. T., B. Raubenheimer, R. T. Guza, and R. A. Holman (1995), Runup kinematics on a natural beach, *J. Geophys. Res.*, *100*(C3), 4985–4993.

Holman, R. A., and A. J. Bowen (1982), Bars, bumps, and holes: Models for the generation of complex beach topography, *J. Geophys. Res.*, *87*(C1), 457–468.

Holman, R. A., and A. H. Sallenger (1985), Set-up and swash on a natural beach, *J. Geophys. Res.*, *90*(C1), 945–953.

Howd, P., A. J. Bowen, and R. A. Holman (1992), Edge waves in the presence of strong longshore currents, *J. Geophys. Res.*, *97*(C7), 11,357–11,371.

Huntley, D. A., R. T. Guza, and A. J. Bowen (1977), A universal form for shoreline run-up spectra?, *J. Geophys. Res.*, *82*(C18), 2577–2581.

Huntley, D. A., R. T. Guza, and E. B. Thornton (1981), Field observations of surf beat: 1. Progressive edge waves, *J. Geophys. Res.*, *86*(C7), 6451–6466.

Inman, D. L., and R. T. Guza (1982), The origin of swash cusps on beaches, *Mar. Geol.*, *49*, 133–148.

Mase, H. (1988), Spectral characteristics of random wave runup, *Coastal Eng.*, *12*, 175–189.

Masselink, G., B. J. Hegge, and C. B. Pattiaratchi (1997), Beach cusp morphodynamics, *Earth Surf. Processes Landforms*, *22*, 1139–1155.

Masselink, G., P. Russell, G. Coco, and D. A. Huntley (2004), Test of edge wave forcing during formation of rhythmic beach morphology, *J. Geophys. Res.*, *109*, C06003, doi:10./1029/2004JC002339.

Oltman-Shay, J., and R. T. Guza (1987), Infragravity edge wave observations on two California beaches, *J. Phys. Oceanogr.*, *17*, 644–663.

Oltman-Shay, J., and R. T. Guza (1993), Edge waves on nonplanar bathymetry and longshore currents: A model and data comparison, *J. Geophys. Res.*, *98*(C2), 2495–2507.

Özkan-Haller, H. T., C. Vidal, I. J. Losada, R. Medina, and M. A. Losada (2001), Standing edge waves on a pocket beach, *J. Geophys. Res.*, *106*(C8), 16,981–16,996.

Pawka, S. S. (1983), Island shadows in wave directional spectra, *J. Geophys. Res.*, *88*(C4), 2579–2591.

Raubenheimer, B. (2002), Observations and predictions of fluid velocities in the surf and swash zones, *J. Geophys. Res.*, *107*(C11), 3190, doi:10.1029/2001JC001264.

Raubenheimer, B., and R. T. Guza (1996), Observations and predictions of run-up, *J. Geophys. Res.*, *101*(C11), 25,575–25,587.

Reniers, A. J. H. M., J. A. Roelvink, and E. Thornton (2004), Morphodynamic modeling of an embayed beach under wave group forcing, *J. Geophys. Res.*, *109*, C01030, doi:10.1029/2002JC001586.

Ruessink, B. G., M. G. Kleinhans, and P. G. L. Van den Beukel (1998), Observations of swash under highly dissipative conditions, *J. Geophys. Res.*, *103*(C2), 3111–3118.

Russell, P. E. (1993), Mechanisms for beach erosion during storms, *Cont. Shelf Res.*, *13*, 1243–1265.

Ursell, F. (1952), Edge waves on a sloping beach, *Proc. R. Soc. London, Ser. A*, *214*, 79–97.

Werner, B. T., and T. M. Fink (1993), Beach cusps as self-organized patterns, *Science*, *260*, 968–971.

Wu, C., E. B. Thornton, and R. T. Guza (1985), Waves and longshore currents: Comparison of a numerical model with field data, *J. Geophys. Res.*, *90*(C3), 4951–4958.

K. R. Bryan, Coastal Marine Group, Department of Earth Sciences, Private Bag, 3105, University of Waikato, Hamilton, New Zealand. (kbryan@waikato.ac.nz)

Y. Ciriano, Departament de Física Aplicada, Escola Politécnica Superior de Castelldefels, Universitat Politècnica de Catalunya, Av. Canal Olímpic, s/n, 08860 Castelldefels (Barcelona), Spain. (yolanda@fa.upc.es)

G. Coco, National Institute of Water and Atmospheric Research, P.O. Box 11-115, Hamilton, New Zealand. (g.coco@niwa.co.nz)

S. Elgar, Woods Hole Oceanographic Institution, Woods Hole, MA 02543, USA. (elgar@whoi.edu)